Nano Energy 99 (2022) 107366

Contents lists available at ScienceDirect

Nano Energy

journal homepage: www.elsevier.com/locate/nanoen

Bio-inspired soft actuator with contact feedback based on photothermal effect and triboelectric nanogenerator☆

Xu Jin [a,b], Yapeng Shi [b,c], Zhihao Yuan [a,b], Xiaoqing Huo [b,c], Zhiyi Wu [b,c,*], Zhong Lin Wang [a,b,c,d,**]

[a] Center on Nanoenergy Research, School of Physical Science and Technology, Guangxi University, Nanning 530004, PR China
[b] Beijing Institute of Nanoenergy and Nanosystems, Chinese Academy of Sciences, Beijing 100083, PR China
[c] College of Nanoscience and Technology, University of Chinese Academy of Sciences, Beijing 100049, PR China
[d] School of Materials Science and Engineering, Georgia Institute of Technology, Atlanta, GA 30332-0245, USA

ARTICLE INFO

Keywords:
Photothermal effect
Environmental robustness
Shape memory
Triboelectric nanogenerators
Contact feedback

ABSTRACT

The development of film soft actuators with contact feedback and outstanding environmental robustness is desirable. In this work, a film-based soft actuator laminated by polyethylene glycol terephthalate (PET), carbon black ink, and polydimethylsiloxane (PDMS) is proposed. Due to the enormous difference in thermal expansion coefficients between these materials, the actuator achieves a large bending deformation angle and a high response speed. Without the shape-memory materials, the actuator can return to its original shape under light-induced after being subjected to mechanical stress. Meanwhile, the actuator maintains its shape after being exposed to extreme temperatures of up to 200 °C and immersion in a variety of solvents. Furthermore, based on the triboelectric effect, the actuator can generate remarkable real-time electrical signals when it mimics the tongue of frogs, bends deformation, and simulates mechanical grippers. This work demonstrates a simple method for building various intelligent and flexible electronic devices and provides promising applications for soft robots.

1. Introduction

Soft robots, without rigid arms and complicated mechanical structures, have a series of merits of flexible, shape-programmable, and stimuli-responsive, which have attracted much attention. According to the new materials and the development of advanced fabrication techniques, soft robots could mimic different locomotive actuations of animals, such as walking, crawling, and jumping [1,2]. Meanwhile, soft robots can respond to various environmental stimuli such as light [3–5], humidity gradients [6–8], chemical gradients [9,10], and temperature changes enabling them to be used in artificial muscles [11], smart systems [7,12], biomimetic devices [13] to perform complex movements. However, the adaptability to the environment, movement feedback, and environment feedback are usually ignored, which is critically considered in the application of soft robots.

In recent years, the development of soft actuators has made great progress in larger drives and faster responses. On the one hand, the actuation force could be enhanced by increasing the rigidity of the actuator material [14,15], which would have a great influence on the bending curvature. On the other hand, the improved response of the soft actuators could be obtained by reducing the response time of volume change [10,14], increasing the absorption/desorption of vapor molecules of the actuator film [7,10,14], increasing the water-induced of the film [16,17], and increasing the light and heat absorption of the film via using carbon nanomaterials [4,18]. For example, Liu et al. proposed a three-layered photothermal actuator with a cooling layer, achieving a fast response under small temperature changes by an additional water evaporation layer for cooling and volume shrinkage on a passive layer [16]. Chen et al. developed a rolled carbon nanotube (CNT)/polydimethylsiloxane (PDMS) bilayer actuator, which could realize the

☆ "Prof Zhong Lin Wang, an author on this paper, is the Editor-in-Chief of Nano Energy, but he had no involvement in the peer review process used to assess this work submitted to Nano Energy. This paper was assessed, and the corresponding peer review managed by Professor Chenguo Hu, also an Associate Editor in Nano Energy".

* Corresponding author at: Beijing Institute of Nanoenergy and Nanosystems, Chinese Academy of Sciences, Beijing 100083, PR China.
** Corresponding author at: Center on Nanoenergy Research, School of Physical Science and Technology, Guangxi University, Nanning 530004, PR China.
E-mail addresses: wuzhiyi@binn.cas.cn (Z. Wu), zlwang@gatech.edu (Z.L. Wang).

https://doi.org/10.1016/j.nanoen.2022.107366
Received 30 March 2022; Received in revised form 23 April 2022; Accepted 7 May 2022
Available online 13 May 2022

imitation of jumping by the excellent photo-thermal effect of CNT and the large difference thermal expansion coefficient between the two layers [19].

Despite this great progress, the mechanical stress, decomposition, oxidation, absorption, and desorption still restrict the environmental robustness of the film soft actuators [3,17,20–24]. Furthermore, the exposed active materials would pose significant challenges to actuators used in the motion or environment feedback. Some groups proposed some solutions to these problems. Fang et al. reported a hierarchical porous structure actuator that is composed of conjugated ladder polymer and CNT, exhibiting high stability, fast absorption and desorption of organic vapor, and a high response rate [9]. Ho et al. proposed a thermo-mechano-electrical transduction actuator, which could harvest thermo-mechanical energy at the mechanistic principles of pyro/piezoelectric effects [25]. Despite the fact that a large number of film soft actuators have been reported in recent years, the development of new types of soft actuators with high environmental robustness, resistance to mechanical deformation, and information feedback is still urgently needed and highly desired for the next-generation flexible electronic devices. Based on triboelectrification and electrostatic induction, originated from Maxwell's displacement current [26], triboelectric nanogenerators (TENGs) are widely applied in self-powered sensors [27–32] and energy harvesters [33]. The TENG-based technology with merits of large design flexibility, simple structure [34], lightweight [35], abundant choice of materials [36], and low cost [37] provides a new strategy for developing self-feedback actuators.

In this work, a soft actuator with great environmental robustness and remarkable contact feedback is constructed, which is composed of a polyethylene terephthalate (PET) film, carbon black ink, and polydimethylsiloxane. According to the screen printing of ink on PET film, the bending direction of this PET-carbon black ink-PDMS actuator (PCPA) can be controlled by the direction stress during the screen-printing process. Benefiting from the large difference in thermal expansion coefficient among the three layers, the PCPA exhibits light-induced fast response and large deformation. Moreover, the PCPA presents outstanding environmental adaptability with high working stability after harsh environmental conditions treatment including up to 200 ℃ and a variety of chemical attacks, which is decided by the PET and the PDMS. Interestingly, the PCPA shaped by molds can achieve the effect of mechanical memory without shape-memory materials. Finally, inspired by the frog tongue, a curly PCPA as a self-powered sensor is presented, which can generate remarkable electrical feedback during the contact process with the other objects. A mechanical gripper with contact feedback is also fabricated, which can grab and manipulate a light sponge. Above all, this PCPA with great environmental robustness and remarkable contact feedback provides an innovative and feasible strategy for the application of soft robots.

2. Results and discussion

2.1. Composition and working illustration of the PCPA

According to the TENGs, when actuators come into contact with other objects, charges are transferred between their surfaces and an obvious electrical signal could be captured by an external circuit. CNT, graphene oxide (GO), or carbon black as widely used materials in soft actuators, exhibit the advantages of the photothermal effect and the electrical conductivity, which promotes TENGs can be easily applied in the soft actuator's tactile feedback process. During the contact process, the TENG based PCPA could generate electrical signals with unique features for different materials, providing innovative strategy and promising prospects for the environment information feedback and motion self-feedback of soft actuators (Fig. 1a).

As depicted in Fig. 1b, the PCPA is assembled layer by layer through screen printing of carbon black ink and spin coating of PDMS with a simple heating method, where a PET film is selected as a passive layer,

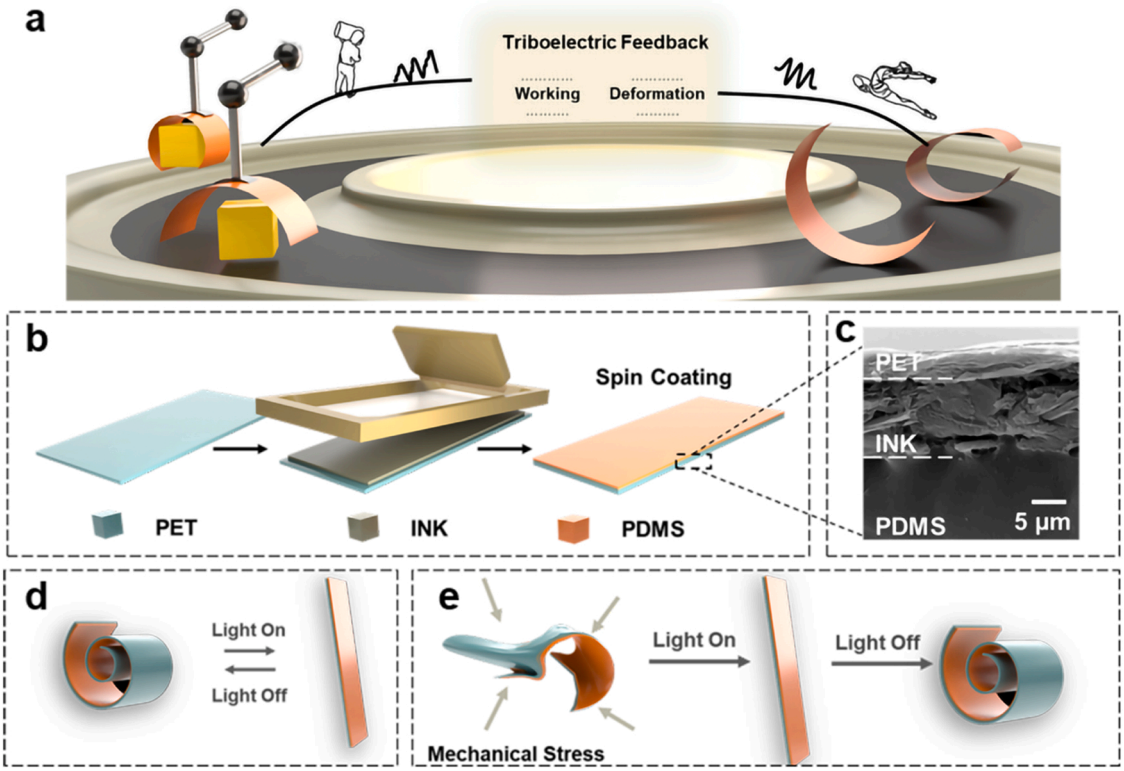

Fig. 1. Fabrication and characterization of the PCPA film. (a) Schematic of the contact feedback of the PCPA. (b) Scheme for fabricating the PCPA actuator. (c) The cross-section SEM image of the PCPA actuator. (d) Schematic illustration of the actuation of the PCPA actuator induced by the light. (e) Schematic illustration of the shape memory of the PCPA actuator.

the carbon black ink layer with remarkable electrical, optical, thermal properties is used to absorb a broad spectrum of light and convert it to heat, and the PDMS layer is specified as the thermal expansion layer. In the processing of screen printing, the direction of the brush has huge influences on the bending directions of the PCPA (Fig. S1), the printing screen meshes can adjust the thicknesses of the ink layer, and the size of the PCPA is decided by the design of the printing screen. PDMS is a kind of silicone elastomer with a large thermal expansion coefficient ($\sim 3 \times 10^{-4}$ K^{-1}) [19], which is much larger than that of ink ($\sim 106 \times 10^{-6}$ K^{-1}) and PET ($\sim 40 \times 10^{-6}$ K^{-1}) [16]. The PCPA bends toward the PDMS side at room temperature, due to the difference in thermal expansion coefficients, the PCPA will bend toward the PET side under the light-induced.

According to the cross-section scanning electron microscopy (SEM) Fig. 1c of the PCPA, the connection of these three layers is relatively tight, and the mechanical characterization of the PCPA exhibits a breaking strength of 4.2 Mpa and a breaking strain of 32% showing great connectivity and flexibility (Fig. S2). The ink layer is fully enveloped with PET and PDMS, ensuring remarkable stability in harsh environments. Meanwhile, the PDMS material with robust physical properties could effectively shield the PCPA from mechanical stress, ensuring the outstanding mechanical memory characteristics of the PCPA without shape-memory materials (Fig. 1d-e).

2.2. The bending deformation performance of the PCPA

Specifying the horizontal direction as the reference position (Fig. S3), the bending deformation performance of the PCPA is calculated at a vertical state, which is closely related to the thickness of each layer and the curing temperature of the PDMS layer. The bending deformation angle of the PCPA decreases from 1080° to 420° as the thickness of the ink layer increases from 5 μm to 30 μm (Fig. S4a, the size of PET film is 4 cm × 1 cm ×2 μm, the thickness of PDMS is 50 μm, and the curing temperature of PDMS is set as 150 ℃). When selecting the thickness of the ink layer as 5 μm (Fig. S4a), the PCPA achieves excellent bending deformation. In addition, when the thickness of the ink layer increases from 5 μm to 8 μm, the resistance value decreases rapidly (Fig. S4b, c), and then the conductivity increases slowly as the thickness increases from 8 μm to 30 μm. Considering that the deformation performance and conductivity have influences on the electrical signal of the PCPA, the thickness of the ink layer is selected as 8 μm. Similarly, the bending deformation angle of the PCPA decreases from 930° to 180° as the thickness of the PDMS layer increases from 23 μm to 300 μm (the thickness of ink layer is 8 μm, and the curing temperature of PDMS is set

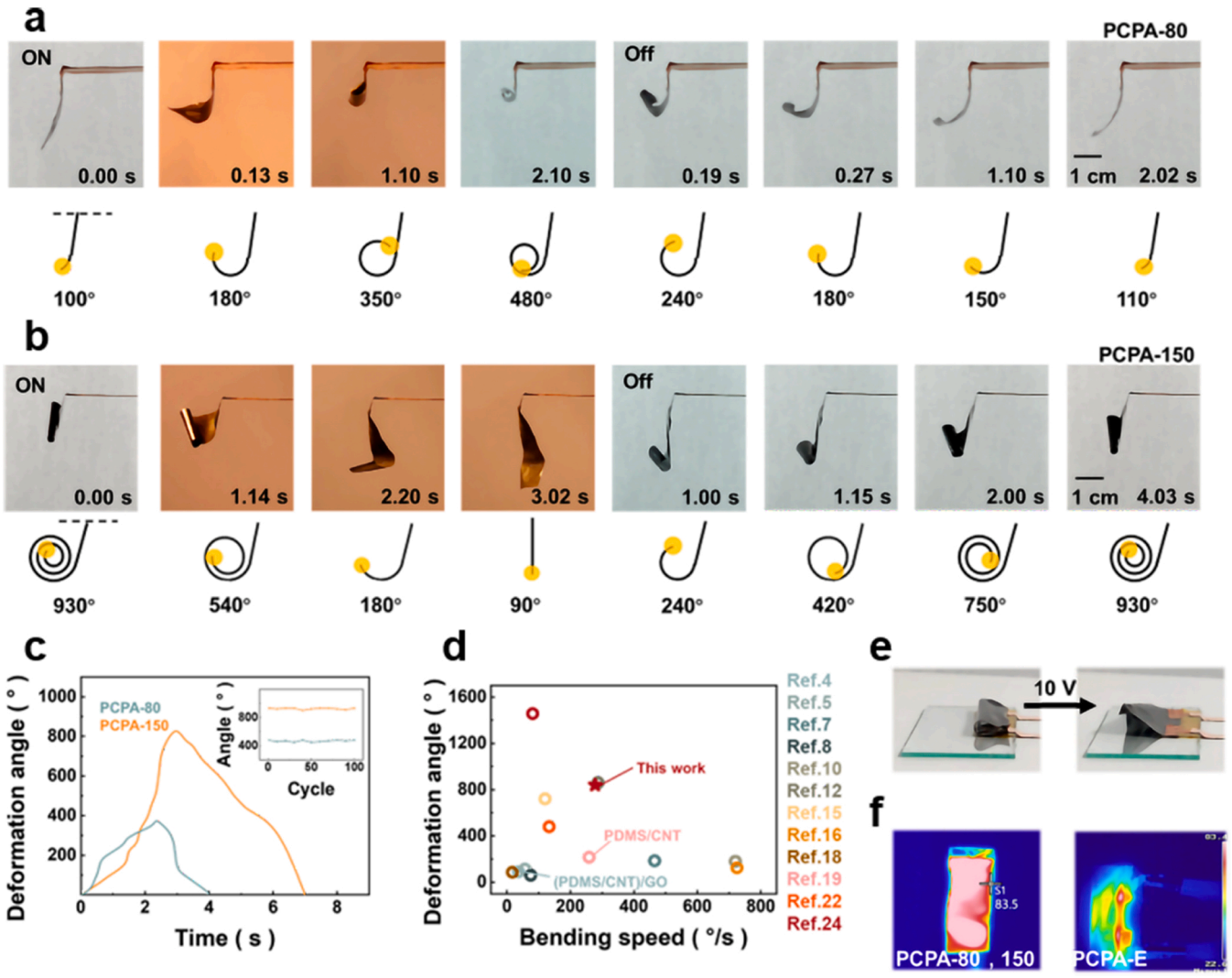

Fig. 2. Actuation performance of the PCPA. (a-b) Photographs of the PCPA-80 and PCPA-150 in different states during a light-induced cycle. (c) The time dependence of the bending deformation angle of the PCPA-80 and PCPA-150. The inset shows the cycling performance of them. (d) Comparison of the response speed and response time of the PCPA with other typical actuators in the previous work. (e) Photographs of the PCPA in different states during the electrical stimulation. (f) Infrared thermal images of the PCPA and PCPA-E.

as 150 ℃. Fig. S5a). Fig. S5b exhibits the time dependence of the bending deformation angle with different thicknesses of PDMS (23 μm, 40 μm, and 65 μm). Because the driving force generated by thermal expansion and the heat conduction are both influenced by the thickness, the PCPA with PDMS of 40 μm has the fastest response time and the shortest deformation period, so the thickness of the PDMS layer is selected as 40 μm in this work. Additionally, the bending deformation of the PCPA is greatly influenced by the curing temperature of the PDMS layer. As the curing temperature decreased from 150 °C to 80 °C, the shape of the PCPA changes from the bending state to the straight state (Fig. S6a), which is attributed to the reduced connectivity and the appearance of the gap between the ink layer and the PDMS layer as the curing temperature reduces (Fig. S6b-c).

Due to the photothermal effect, the ink layer of the PCPA would absorb light and convert it into heat, and then the PDMS layer generates volume expansion, causing the PCPA to bend to the PET side. The bending performance of the PCPA-80 (the PDMS layer of the PCPA is cured at 80 °C, the PET side toward the left) under light is shown in Fig. 2a and Movie 1. The PCPA-80 (4 cm × 1 cm × 50 μm) can bend by 380° in 2.10 s when it is exposed to light, which corresponds to a bending deformation angle of 9.5°/mm and a bending speed of 181°/s, and it will unbend in 2.02 s. Contrarily, the PCPA-150 (the PDMS side toward the left) can unbend by 840° in 3.02 s when it is exposed to light, which corresponds to a bending deformation angle of 21° and a bending speed of 278°/s, and it will unbend in 4.03 s (Fig. 2b). The time dependence of the bending deformation angle of the PCPA-80 and the PCPA-150 is shown in Fig. 2c and the inset shows the steady cycling performance of the two samples. In the previous work, there is a large number of typical film soft actuators (Fig. 2d). The large deformation angle and high response speed can be obtained via different strategies for developing delicate material and structural designs. The folded-GO actuator [24], which exhibits actuation speeds of 81°/s and 1456° deformation angle, is made by the three-dimensional shrinking method to induce a highly folded GO surface. The gradient porous structure actuator [15] can achieve 720° bending angle and 120°/s actuation speeds, which is built up through ammonia-triggered electrostatic complexation of a poly(ionic liquid) with poly(acrylic acid). The cross-linked LC polymers actuator [7] can exhibit actuation speeds of 465.5°/s and 185° deformation angle, which is using the hydration of oxygen-containing groups and LCs alignment. The PDMS-base actuators, CNT/PDMS [19] and GO/CNT/PDMS [4], exhibit the actuation speeds of 259°/s and 36.29°/s, respectively, which are driven by photothermal aided water evaporation from the film. Compared with the above design strategies, this work presents a laminated construction actuator with a

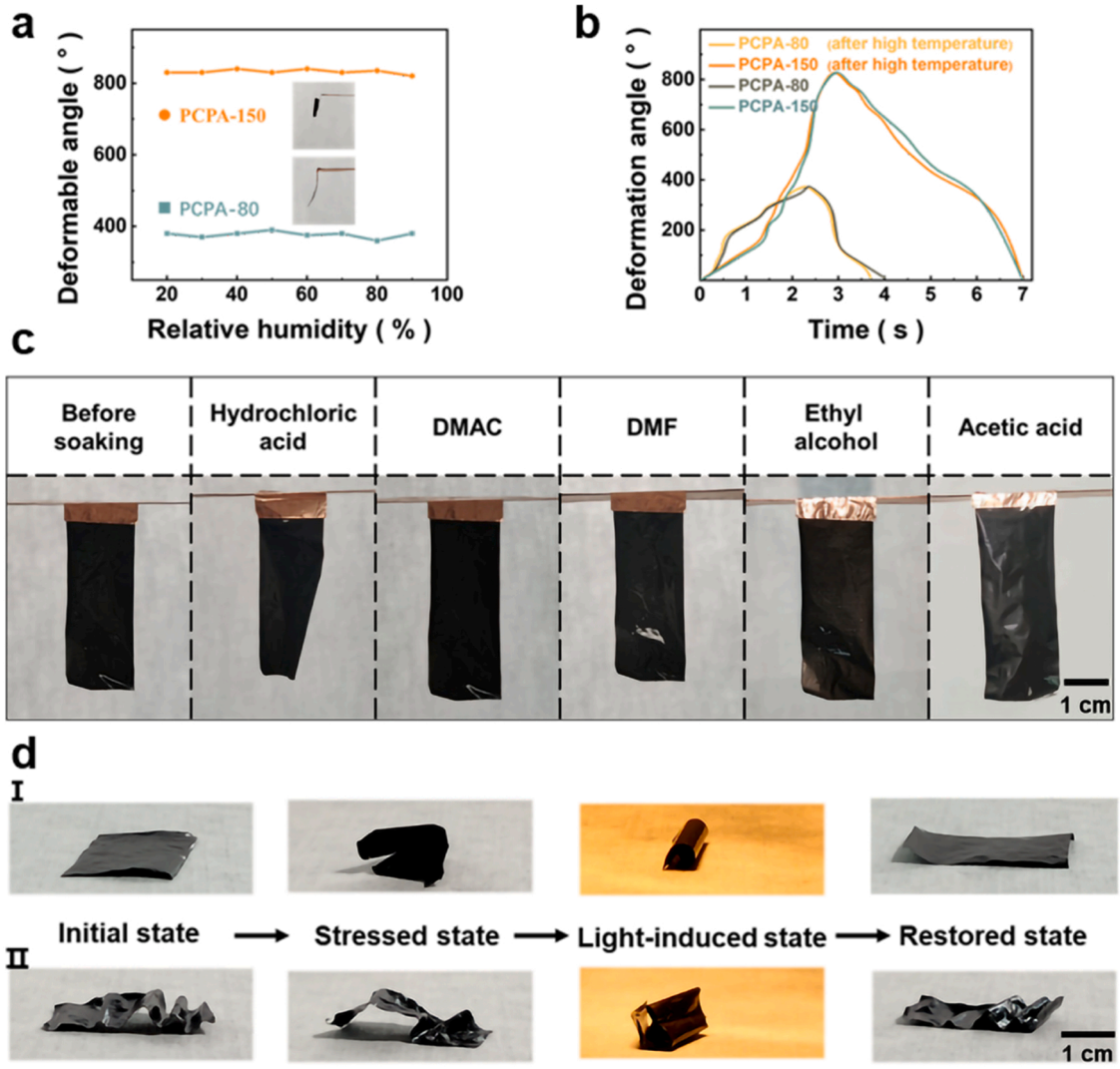

Fig. 3. The environmental adaptability and shape memory diversity of PCPA. (a) The curvature of the PCPA at different RHs. (b) The time dependence of the bending curvatures of the PCPA-80 and PCPA-150 after high temperature. (c) Photographs of PCPA after soaking in different solvents. (d) Photographs of PCPA demonstrating the shape memory diversity.

bending angle of 840°and an actuation speed of 278°/s. Meanwhile, due to the polymer material cladding structure, the PCPA demonstrates high tolerance to harsh environments, which will be discussed in the following sections. In addition to the light-induced, the PCPA could also be driven by electricity based on the Joule heat effect (PCPA-E). As demonstrated in Fig. 2e, the PCPA can unbend by 180° in 6.3 s under a voltage of 10 V. It is worth noting that the intensity of stimulus will affect the response. The infrared images (Fig. 2f) and Movie 2 demonstrate the surface temperature changes of the PCPA under electrical stimulation and light-induced, respectively.

Supplementary material related to this article can be found online at doi:10.1016/j.nanoen.2022.107366.

2.3. The robustness of the PCPA

The ability to work stably under various extreme environmental conditions for intelligent soft actuators is essential including high humidity, high temperature, harsh chemical environment, etc. PET and PDMS have remarkable environmental robustness, protecting the PCPA against high humidity, high temperature, some organic solvents, or

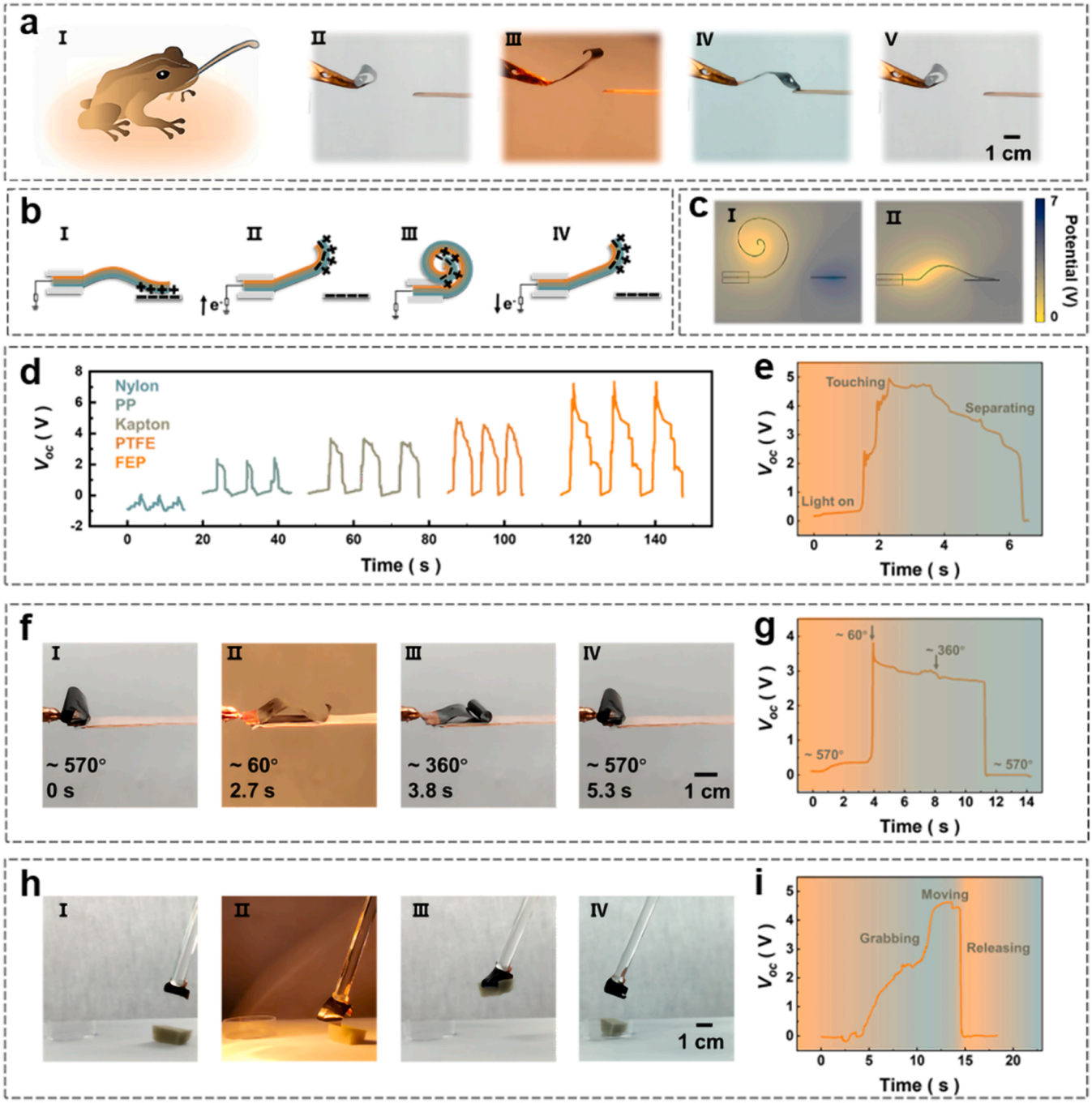

Fig. 4. The contact feedback performance of the PCPA. (a) Schematic illustration and corresponding photographs of the PCPA-130 during the imitation process of the frog-tongue. (b) The schematic diagram of the electricity generation process in a full cycle of the PCPA. (c) The simulation results of electrostatic potential distributions of the PCPA by COMSOL. (d) The different V_{oc} with the unique features by the PCPA during the contact-separation process with various materials. (e) The open-circuit voltage (V_{oc}) feature generated by the PCPA (contact PTFE). (f) Photographs of PCPA unbend on a surface and (g) electrical feedback. (h) Photographs of light-induced mechanical gripper for manipulating sponge. (i) The electrical contact-feedback of mechanical gripper during the manipulating process.

corrosive solutions. Fig. 3a shows the PCPA keeps the stability of bending deformation angle under different humidity, and the deformation angle is relatively invariable with no obvious fluctuation. Furthermore, the PCPA (1 cm × 1 cm × 50 μm) could straighten to 180° immediately when it is immersed in 80 ℃ water (Fig. S7), further indicating the prominent working properties in high humidity. Moreover, the PCPA can maintain its shape and keep the great performance of bending deformation at the room temperature (25 ℃) after being heated to 200 ℃ with a certain heating rate of 10 ℃/min and then cooled to 25 ℃ (Fig. 3b). In addition, a range of solutions including 1 mol/L hydrochloric acids, dimethylacetamide (DMAC), Dimethylformamide (DMF), ethyl alcohol, and acetic acid are utilized to investigate the solvents tolerance of the PCPA-80. Firstly, the PCPA-80 is immersed in every solvent mentioned above for 5 min at room temperature, then rinsed with deionized water, and dried. The shape of the PCPA does not change significantly (Fig. 3c), meanwhile, the deformation angle and the actuation speed have no obvious degradation (Fig. S8). However, since the PET layer and the PDMS layer are not stable in the highly acidic solvent, basic solvent, and some other solvents, the solvents tolerance of the PCPA is also limited to some extent.

Considering that the soft actuators may face mechanical stress, the shape memory ability of the PCPA is indispensable. Benefiting from the remarkable mechanical robustness of the PDMS, the PCPA could recover to the original shape under light-induced after being subjected to mechanical stress without adding shape-memory materials in the fabrication process, and it can maintain the deformation performance under light-induced (Movie 3). The PCPA-80 can endure mechanical stress in random directions, bend under light-induced, and then return to the initial state after the light is off (Fig. 3dI). Based on the remarkable plasticity of PDMS, a wavy-like PCPA-80 with extraordinary shape memory ability is obtained by using a handmade mold during the curing processing of PDMS (Fig. S9), demonstrating the shape memory diversity of soft actuator (Fig. 3dII).

Supplementary material related to this article can be found online at doi:10.1016/j.nanoen.2022.107366.

2.4. The contact feedback of the PCPA

The feedback mechanism is a great challenge for film soft actuators because of the size. TENG, as a kind of self-powered sensor, could generate special electrical signals during the contact process of the other materials, which provides an innovative and feasible strategy for the contact-feedback mechanism of soft actuators. It is promising that the soft actuators with the ability of contact-feedback will be more widely applied if the soft actuator and TENG are integrated. Inspired by the frog-tongue, a tool of the frog to hunt by straightening and curling (Fig. 4aI), the PCPA-130 could successfully mimic the predation process of the frog under light-induced (Fig. 4aII-V and Movie 4). By fixing one side of the PCPA-130 (4 cm × 1 cm × 50 μm), the PCPA-130 could straighten by 570° in 3 s under light, and the generated high actuation stress will make the other side of the PCPA launch and contact with external objects, then generate obvious electrical signals. The whole straighten-curl process lasts only 10 s, due to the preeminent photothermal properties of the PCPA. As illustrated in Fig. 4b, when the PCPA moves to contact the object, the equivalent number of static charges with opposite polarities will be generated at the contacting interfaces. Taking polytetrafluoroethylene (PTFE) as the counter material, for example, the surface of the PCPA (PET) will be positively charged. When the PCPA is separated from the object, the negative charges in the conductive ink will be induced to balance the local charge at the ink/PET interfaces, and electrons move from the ground to the ink/PET interfaces. Therefore, currents flow from the ink electrode to the ground through the external circuit. The current will stop when the PCPA is far away and the static charges in PCPA are all screened Fig. 4b III. When the PCPA approaches the object again, charges will flow in the opposite directions (Fig. 4b IV). Fig. 4c describes the potential simulation results of the PCPA in the contact feedback processing by using the COMSOL Multiphysics. In addition, due to the different charge transferability of these materials, the generated electrical signals are different with unique features, which make it possible for the PCPA to realize the material identification by machine learning. Fig. 4e exhibits five characteristics of open-circuit voltage (V_{oc}) waveforms of the PCPA during the contact-separation process with nylon, polypropylene (PP), Kapton, PTFE, and fluorinated ethylene propylene (FEP). As shown in Fig. 4d, there are obvious potential changes (5 V) in the contact-separation process between the PCPA and PTFE (Fig. S10).

Supplementary material related to this article can be found online at doi:10.1016/j.nanoen.2022.107366.

In addition, the PCPA achieves motion self-feedback on a PTFE plane under light-induced. The contact area between the PTFE and the PCPA increases when the PCPA unbends (Fig. 4f), increasing the potential between the ground and the PCPA. The PCPA generates a strong electric signal (3.7 V) when the PCPA rapidly contacted the PTFE plane. After removing the light-induced, the PCPA constantly curls to about 360°, then most of the PCPA separates from the PTFE plane and the electrical signal drops to 0 V. The whole process and real-time feedback are shown in Movie 5, which shows monitoring the status of the PCPA feasible and easy. Meanwhile, the PCPA can keep the electrical performance stable for 100 cycles (Fig. S11). Finally, the PCPA-130 is successfully applied as a mechanical gripper to grab and manipulate a piece of sponge (10 mm × 10 mm × 20 mm, 18 mg) under light-induced (Fig. 4h and Movie 6). The gripper will open when the light is applied (Fig. 4hII), and then curls to grab the sponge when the light is off (Fig. 4hIII). After that, the sponge is picked up and moved to another place, then turn on the light, and the gripper will straighten to release the sponge (Fig. 4hIV). The voltage waveform of the whole process is presented in Fig. 4i. By the effective combination of the PCPA and TENG, the soft actuators can successfully realize contact feedback with a more environmental application, which provides a new strategy for the innovation of intelligent and convenient soft robots.

Supplementary material related to this article can be found online at doi:10.1016/j.nanoen.2022.107366.

3. Conclusion

In summary, a robust thin-film soft actuator is fabricated by laminating PET, carbon black ink, and PDMS to achieve great environmental robustness, distinguished shape-memory characteristics, and outstanding contact feedback. Due to the enormous difference in thermal expansion coefficients between these materials, the soft actuator exhibits a huge bending deformation angle of 840° and a high response speed of 278°/s. The soft actuator can maintain its shape and keep bending performance after being exposed to a variety of harsh environments including high temperature (200 ℃), high humidity, and some organic solvents because of the protection of PET and PDMS. Meanwhile, the actuator can achieve the remarkable shape memory characteristic without shape-memory materials and can be shaped by molds. Furthermore, based on the triboelectric effect, the soft actuator as a self-powered contact sensor realizes remarkable contact feedback when it mimics the frog-tongue, deforms, and simulates a mechanical gripper. This design is conducive to the development of intelligent soft robots, flexible electronic devices, and sensors for detectors, controllers, and other biomimetic applications.

4. Experimental section

4.1. Fabrication of the PCPA

The ink is commercially available (TJ-1830, Tengjing Electronic Materials Co. Ltd, Shenzhen, China.), which is composed of carbon black (3 −5%), polyurethane (30%) in the mixed solvents of ethyl acetate and acetone (20%/80%) provided by the supplier. The ink is coated on PET

with 400 mesh silkscreens, then held at 150 ℃ for 30 min. And densify the ink layer with ethanol after it cooled down. The PDMS (Sylgard 184 silicone elastomer, from Dow Corning) is commercially purchased. The PDMS prepolymer was mixed with a curing agent (10:1 by weight) and cured at 150 °C for 30 min **The TENG based PCPA**. The ink is coated on PET and held at 150 ℃ for 10 min, a copper foil is added to the edge of the ink layer, then, the ink is held at 150 ℃ for 20 min to completely dry. Finally, the PDMS is spined on the ink layer to cover the ink and the electrode.

4.2. Characterization

Light-induced actuation is measured from the pictures recorded by a digital camera in OnePlus 8. The thickness of the films is measured by a portable thickness gauge from EVERTE. Infrared images as well as the temperature variation in light-induced actuation are tested by the thermal infrared imager (KEYSIGHT U5857A). The SEM images were obtained by TESCAN MIRA LMS field emission scanning electron microscope. The electrical output performance of the PCPA is measured by using an electrometer (KEITHLEY Model 6514 system electrometer), a data acquisition card (NI PCIe-6376).

CRediT authorship contribution statement

Xu Jin conceived the idea and fabricated the actuator. Yapeng Shi performed the SEM characterizations and Supplementary Movies. Zhihao Yuan and Xiaoqing Huo provided some suggestions on fabricating the devices and electrical measurement. Zhiyi Wu and Zhong Lin Wang supervised the project. All authors discussed the results and contributed to the writing of the paper.

Declaration of Competing Interest

The authors declare that they have no known competing financial interests or personal relationships that could have appeared to influence the work reported in this paper.

Acknowledgements

The authors thank the support of the National Natural Science Foundation of China (61503051).

Appendix A. Supporting information

Supplementary data associated with this article can be found in the online version at doi:10.1016/j.nanoen.2022.107366.

References

[1] J.J. Li, X. Zhou, Z.F. Liu, Recent advances in photoactuators and their applications in intelligent bionic movements, Adv. Opt. Mater. 8 (2020), 2000886.
[2] M. Li, N.A. Ostrovsky-Snider, M. Sitti, F.G. Omenetto, Cutting the cord: progress in untethered soft robotics and actuators, MRS Adv. 4 (2019) 2787–2804.
[3] X. Zhang, Z. Yu, C. Wang, D. Zarrouk, Photoactuators and motors based on carbon nanotubes with selective chirality distributions, Nat. Commun. 5 (2014) 2983.
[4] W. Wang, C. Xiang, Q. Zhu, W. Zhong, Multistimulus responsive actuator with GO and carbon nanotube/PDMS bilayer structure for flexible and smart devices, ACS Appl. Mater. Interfaces 10 (2018) 27215–27223.
[5] L. Zheng, H. Li, W. Huang, X. Lai, Light stimuli-responsive superhydrophobic films for electric switches and water-droplet manipulation, ACS Appl. Mater. Interfaces 13 (2021) 36621–36631.
[6] P. Zhou, L. Chen, L. Yao, M. Weng, Humidity- and light-driven actuators based on carbon nanotube-coated paper and polymer composite, Nanoscale 10 (2018) 8422–8427.
[7] Y. Liu, B. Xu, S. Sun, J. Wei, Humidity- and photo-induced mechanical actuation of cross-linked liquid crystal polymers, Adv. Mater. 29 (2017).
[8] C. Lv, H. Xia, Q. Shi, G. Wang, Sensitively humidity-driven actuator based on photopolymerizable PEG-DA films, Adv. Mater. Interfaces 4 (2017).
[9] K. Yu, X. Ji, T. Yuan, Y. Cheng, Robust jumping actuator with a shrimp-shell architecture, Adv. Mater. (2021), e2104558.
[10] J. Mu, G. Wang, H. Yan, H. Li, Molecular-channel driven actuator with considerations for multiple configurations and color switching, Nat. Commun. 9 (2018) 590.
[11] M. Kanik, S. Orguc, G. Varnavides, J. Kim, Strain-programmable fiber-based artificial muscle, Science 365 (2019) 145–150.
[12] L. Zhang, P. Naumov, X. Du, Z. Hu, Vapomechanically responsive motion of microchannel-programmed actuators, Adv. Mater. 29 (2017).
[13] H. Shahsavan, A. Aghakhani, H. Zeng, Y. Guo, Bioinspired underwater locomotion of light-driven liquid crystal gels, Proc. Natl. Acad. Sci. USA 117 (2020) 5125–5133.
[14] Q. Zhao, J.W. Dunlop, X. Qiu, F. Huang, An instant multi-responsive porous polymer actuator driven by solvent molecule sorption, Nat. Commun. 5 (2014) 4293.
[15] H. Lin, J. Gong, H. Miao, R. Guterman, Flexible and actuating nanoporous poly (Ionic Liquid)-paper-based hybrid membranes, ACS Appl. Mater. Interfaces 9 (2017) 15148–15155.
[16] J.J. Li, R. Zhang, L.L. Mou, M.J. de Andrade, Photothermal bimorph actuators with in-built cooler for light mills, frequency switches, and soft robots, Adv. Funct. Mater. 29 (2019).
[17] X.K. Wang, L.L. Li, E.P. Liu, J.J. Wang, High-performance multiresponsive bilayer actuators based on micro-/nanostructured polypyrrole for robust smart devices, ACS Appl. Nano Mater. 4 (2021) 5349–5359.
[18] D.C. Hua, X.Q. Zhang, Z.Y. Ji, C.Y. Yan, 3D printing of shape changing composites for constructing flexible paper-based photothermal bilayer actuators, J. Mater. Chem. C. 6 (2018) 2123–2131.
[19] Y. Hu, J.Q. Liu, L.F. Chang, L.L. Yang, Electrically and sunlight-driven actuator with versatile biomimetic motions based on rolled carbon nanotube bilayer composite, Adv. Funct. Mater. 27 (2017), 1704388.
[20] J. Mu, C. Hou, H. Wang, Y. Li, Origami-inspired active graphene-based paper for programmable instant self-folding walking devices, Sci. Adv. 1 (2015), e1500533.
[21] L. Chen, M. Weng, P. Zhou, L. Zhang, Multi-responsive actuators based on a graphene oxide composite: intelligent robot and bioinspired applications, Nanoscale 9 (2017) 9825–9833.
[22] Y. Hu, G. Wu, T. Lan, J. Zhao, A. Graphene-Based, Bimorph structure for design of high performance photoactuators, Adv. Mater. 27 (2015) 7867–7873.
[23] T.P. Wang, M.T. Li, H. Zhang, Y.Y. Sun, A multi- responsive bidirectional bending actuator based on polypyrrole and agar nanocomposites, J. Mater. Chem. C. 6 (2018) 6416–6422.
[24] Y. Tan, Z. Chu, Z. Jiang, T. Hu, Gyrification-inspired highly convoluted graphene oxide patterns for ultralarge deforming actuators, ACS Nano 11 (2017) 6843–6852.
[25] X.Q. Wang, C.F. Tan, K.H. Chan, X. Lu, In-built thermo-mechanical cooperative feedback mechanism for self-propelled multimodal locomotion and electricity generation, Nat. Commun. 9 (2018) 3438.
[26] Z.L. Wang, On Maxwell's displacement current for energy and sensors: the origin of nanogenerators, Mater. Today 20 (2017) 74–82.
[27] C.M. Boutry, M. Negre, M. Jorda, O. Vardoulis, A hierarchically patterned, bioinspired e-skin able to detect the direction of applied pressure for robotics, Sci. Robot 3 (2018).
[28] H. Guo, X. Pu, J. Chen, Y. Meng, A highly sensitive, self-powered triboelectric auditory sensor for social robotics and hearing aids, Sci. Robot. 3 (2018) eaat2516.
[29] Z. Wu, B. Zhang, H. Zou, Z. Lin, Multifunctional sensor based on translational-rotary triboelectric nanogenerator, Adv. Energy Mater. 9 (2019).
[30] B. Zhang, Z. Wu, Z. Lin, H. Guo, All-in-one 3D acceleration sensor based on coded liquid–metal triboelectric nanogenerator for vehicle restraint system, Mater. Today (2020).
[31] R. Li, X. Wei, J. Xu, J. Chen, Smart wearable sensors based on triboelectric nanogenerator for personal healthcare monitoring, Micro 12 (2021).
[32] O. Yue, X. Wang, X. Liu, M. Hou, Spider-web and ant-tentacle doubly bio-inspired multifunctional self-powered electronic skin with hierarchical nanostructure, Adv. Sci. (2021), e2004377.
[33] X. Jin, Z. Yuan, Y. Shi, Y. Sun, Triboelectric nanogenerator based on a rotational magnetic ball for harvesting transmission line magnetic energy, Adv. Funct. Mater. (2021).
[34] J. Chen, X. Wei, B. Wang, R. Li, Design optimization of soft-contact freestanding rotary triboelectric nanogenerator for high-output performance, Adv. Energy Mater. (2021).
[35] Z. Yuan, X. Wei, X. Jin, Y. Sun, Magnetic energy harvesting of transmission lines by the swinging triboelectric nanogenerator, Mater. Today Energy 22 (2021).
[36] H. Zou, Y. Zhang, L. Guo, P. Wang, Quantifying the triboelectric series, Nat. Commun. 10 (2019) 1427.
[37] P. Cheng, H. Guo, Z. Wen, C. Zhang, Largely enhanced triboelectric nanogenerator for efficient harvesting of water wave energy by soft contacted structure, Nano Energy 57 (2019) 432–439.